

MULTISTAGE CHEMICAL BATH DEPOSITION OF THICK FILM CADMIUM SULFIDE FOR CdS/CdTe X-RAY DETECTOR

H. SHAMS¹, H. ABOU GABAL¹, M. SOLIMAN², S. EBRAHIM², S. AGAMY¹

¹ Nuclear and Radiation Engineering Department, Faculty of Engineering, Alexandria University, Alexandria, Egypt.

² Materials Science Department, Institute of Graduate Studies and Research, Alexandria University, Alexandria, Egypt.

(Corresponding author: Shams.hisham@yahoo.com)

Abstract :- Many methods are used to measure X-ray flux generated by modern X-ray machines. The most common method utilized for monitoring X-ray dose is technically complex and expensive. In this work multilayer of cadmium sulfide (CdS) using chemical bath deposition (CBD) were carried out to deposit thick layer optimum thickness to produce CdS/CdTe junction x-ray detector. It was intended to use simple, available and low cost deposition method to produce low cost detector with very simple circuit to read out the output signal. The effects of the deposition time, cadmium chloride heat treatment, the ammonia and thiourea concentration on CdS layers were controlled and investigated through scanning electron microscope (SEM), energy dispersive x-ray analysis (EDXA), X-ray diffraction (XRD), and ultraviolet (UV)-visible spectroscopy. The XRD analysis showed that the CdS films have highly oriented crystallites with the classical hexagonal structure (wurtzite type) and the main six diffraction peaks. The relatively stronger and narrow peak of CdS film obtained with 6 stages along (002) plane indicated that the film is highly oriented along the c-axis. The band gap E_g can be extrapolated to be 2.41 eV. It was observed that the maximum and the minimum amplitudes of the pulse formed due to exposed FTO/CdS/CdTe/Mo detector to X-ray of 33 keV and 1mA intensity are 0.732 and -0.405 V and consequently the total output amplitude is 1.137 V.

Keywords: CdTe; CdS; Thin film; X-ray; Sensor.

Received: February 1, 2018. Revised: March 8, 2018. Accepted: June 1, 2018. Published: August 1, 2018.

1 Introduction

Deposition of thin chalcogenide films by vacuum evaporation, sputtering and chemical methods are well known and interested in the fabrication of solar selective coatings, solar cell, photoconductors, sensors and detectors [1]. CBD technique is recognized to be a relatively simple, low cost and scalable for the deposition of high quality CdS thin film required by the solar cell industry. CBD has been used in the deposition of CdS semiconductor thin film. CdS as a n-type semiconductor has been used as a window and buffer layer in the fabrication of efficient thin film solar cells based on CdTe or Cu (In,Ga) SeS [2]. Wagner et al prepared CuInSe/CdS heterojunction particle detectors and CdTe was deposited using close-space sublimation. They found that the individual alpha particles were detected with an intrinsic efficiency of >80%, while the junctions were insensitive to gamma rays [5]. Kang et al used

photovoltaic detector for spectroscopy in the visible and near infrared regions. They found that the spectral dependence of the quantum efficiency was bias dependent for diodes with appreciable insulating layers of reverse bias ≥ 2 V or at zero bias for diodes with no insulating layer [3]. Tomita et al fabricated CdS/CdTe heterojunction devices by radio frequency sputter deposition method to be used for x-ray imaging sensors. It was noted that an x-ray imaging camera tube consisting of CdS/CdTe heterojunction photoconductive target had three times larger responses to x-rays than the conventional PbO x-ray tube [4]. Murphy et al fabricated thin film diode based on CdTe with a diameter of up to 3.5 mm to function effectively as single-event charged Monte Carlo simulations to employ deeply penetrating mega-voltage x-rays delivered with linear accelerator and specified the quantity of x-ray exposed using thin film CdS/CdTe then they verified the measurements using fabricated prototype

CdS/CdTe solar cells, which fabricated by the sequential deposition of SnO₂, CdS, CdTe, and a back contact layer. The fabricated prototype has shown remarkable accurate readings of the x-ray beam intensity compared to the MC simulations [6].

There are other different methods have been applied to deposit CdS thin films such as electrodeposition, spray pyrolysis, molecular beam epitaxy, metal organic chemical vapor deposition, successive ionic layer adsorption and reaction, physical vapor deposition and sputtering [7-14]. However, CBD cannot use in the ionizing radiation sensing applications in which thicker and high quality CdS films are required. This is due to the following two reasons. First, the formation of a saturate CdS layer is between 0.05 and 0.2 μm and duplex layer is formed by longer of the deposition time. The duplex layer consists of very adherent inner layer and a less adherent outer layer. Second, the heterogeneous reaction on the substrate surface (increasing the CdS thickness), homogenous reaction in the bulk of the solution (increasing the CdS concentration in the solution) is presented [15]. The main target to this work is to investigate the effect of different deposition parameters of CdS, such as the deposition time, molar concentrations of thiourea and ammonia on the surface morphology, the chemical composition, thickness and the optical property. The multistage deposition of CdS thick film is carried out onto the FTO substrate to overcome the limited thickness. In addition, the performance of thick CdS/CdTe heterojunction as X-ray detector is studied.

2 Materials and Methods

2.1 Materials

Cadmium acetate dihydrate (99%, MW = 266.52 g/mole) was obtained from Merck. Ammonium acetate (98%, MW = 77.08 g/mole) was purchased from Carlo Erba. Ammonia (25%, MW = 17.03 g/mole) was received from Chem. Thiourea (99% MW = 76.12 g/mole) was obtained from Loba Chemi. Cadmium chloride pentahydrate was obtained from Sigma Aldrich. Fluorine doped tin oxide (FTO) coated glass slide with sheet resistance of 7 Ohm/sq was bought from Sigma Aldrich.

2.2 Preparation of thick film of CdS

CdS films were deposited on FTO substrate using a heated alkaline solution of cadmium acetate dihydrate as the Cd²⁺ source, thiourea as the S²⁻ source, ammonium acetate serving as a buffer and ammonia as a complexing agent. CdS films, were prepared using different molar concentrations of thiourea (0.06 - 0.09M) and ammonia (8-11-14M) with 0.03 M cadmium acetate dihydrate and 1M ammonium acetate [16]. The FTO glass substrate was immersed in a solution of cadmium acetate dihydrate, the ammonium acetate and the ammonia and heated with stirring at 88 °C through 30 minutes. The thiourea solution was added dropwise in four aliquots every 10 minutes. After the CdS deposition, the substrate was removed from the bath and placed in warm deionized water. Finally, the substrate was sonicated for about 2 minutes to remove loosely adherent CdS particulates. The treatment of CdS film was achieved by dropping 1 N solution of CdCl₂ in methanol and the films was heated at 350 °C for 15 minutes. The deposition time was varied from 2 to 4 hours. Multistage deposition of CdS thin films was achieved to control the thickness of the films. Six successive layers were deposited by the same conditions.

2.3 Fabrication of CdS/CdTe X-ray detector

CdTe was electrodeposited onto the prepared CdS/FTO substrates. CdTe was deposited using potentiostat Gamry 750G using a two-electrode cell. The system consisting of CdS/FTO working electrode as a cathode and a graphite electrode as an anode immersed in an electrolyte. The electrolyte solution consists of cadmium sulfate 3.8x10⁻²M solution, 4.2x10⁻² M of CdCl₂ and 10⁻³M of TeO₂. The TeO₂ solution was prepared by dissolving 0.032 gm of TeO₂ in 2ml of dilute sulfuric acid and then this solution was added to 200ml of deionized water. The produced heterojunction was treated again with 1 N CdCl₂ at 350°C for 15 min. and was cleaned with distilled water. The cyclic voltammetry was used to provide the optimum applied voltage for CdTe deposition onto CdS/FTO glass substrate, where -1.2 V was found suitable for CdTe film deposition. By growing CdTe layer onto CdS/FTO at constant voltage a homogeneous good distribution layer was established.

Mo metal as a back contact was deposited on CdTe/CdS/FTO heterojunction samples by RF

magnetron sputtering system. The CdTe/CdS/FTO hetero junction samples were subsequently put into the vacuum chamber and placed at a distance of 10 cm from the Mo target. The vacuum chamber was initially evacuated to a base pressure of 8×10^{-5} kPa. Then pure argon flow of 0.094 L²/min was introduced into the chamber to keep the pressure during the film deposition at a value around 1.9×10^{-4} kPa. The power supply was then turned on and adjusted at 60 W. The schematic diagram of the fabricated detector with different layers is shown in Figure (1).

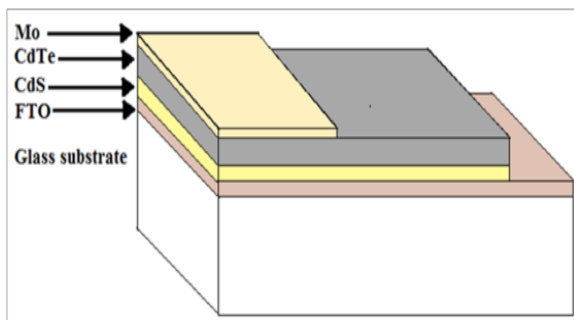


Figure : 1 The structure of the fabricated x-ray detector.

2.4 Characterization techniques

To characterize the deposited CdS films, a scanning electron microscopy QUANTA FEG250 was used to observe the surface morphology and measure the film thickness. The chemical compositions of the films were determined with an Energy dispersive x-ray spectrometer QUANTA FEG250. The crystalline structure was studied by means of x-ray diffraction using (x-ray 7000 Shimadzu-Japan) at room temperature. The Bragg The small particles of CdS are accumulated continuously and covered the entire surface of the substrate to produce a homogeneous CdS layer. This indicates that the homogeneity of the CdS film is better with 4 hrs deposition time. This result is similar to that recorded by Fouad et al [18]. However, we extend the deposition time for 4 hrs to enhance the adhesion and to produce homogeneous and smooth surface. The EDX analyses indicate the atomic percents of S/Cd are 37.16/62.84, 21.45/78.55 and 45.7/54.3 correspond to 2.0, 3.0 and 4.0 hrs, respectively. It is noticed that at 4 hrs depositions

angle (2θ) in the range from 5 to 50 degrees was measured. The x-ray source was Cu target generated at 30 KV and 30 mA with scan speed 4 deg/min. The electronic absorption spectra were obtained using UV-Visible spectrophotometer (Evolution 600 double beams scanning UV-visible spectrophotometer, Thermo scientific, USA) in the range of 200-800nm.

2.5 Performance measurement of CdS/CdTe X-ray detector

X-ray generator Geratogram Roentgen instrument (Germany, 1987) was used to produce an X-ray adjustable energy range of 21 to 42 keV and with an emission current adjustable range of 0.05 to 1 mA with local dose rate at a distance of 0.1m from the touchable surface of the device is $\leq 5 \mu\text{Sv}$. The perpendicular X-ray was incident onto the fabricated CdS/CdTe detectors. The output of four stacked detectors in series was connected to computerized oscilloscope DS03064 Kit V to read the output signal.

3 Results and Discussion

3.1 Surface Morphology and Composition Analysis of CdS Film

3.1.1 Effect of Deposition Time

The influence of the deposition time on the morphology of the CdS films is shown in Figure (2). The formed CdS films Grain growth are clearly noticed from the SEM micrographs of the film deposited at 4 hrs. It has a good adherence to the FTO substrate with a few pinholes. Moreover, the FTO surface is covered with spherical grains and their sizes decrease from 16 to $1.9 \mu\text{m}$ and their densities increase with a long time of deposition.

time, the S/Cd ratio is more stoichiometry than 2 and 3 hrs. This is attributed to the longer time of deposition increasing the number of collisions and the probability of formation of CdS compound [17].

3.1.2 Effect of ammonia concentration

The SEM micrographs of the surface morphology of the CdS films deposited with different ammonia concentrations (14, 11 and 8M) are illustrated in Figure (3). The micrographs reveal that the CdS films are smooth, homogeneous with few cracks and the good distribution of the granules at

low concentration is observed [18]. The small particles accumulate continuously and cover the entire surface of the substrate leading to an homogeneous layer. This indicates that the mechanism film formation is due to ion-by-ion deposition (heterogeneous mechanism). The EDX results of the CdS films prepared with the different ammonium hydroxide concentrations indicate that the atomic percent of S/Cd are 45.7/54.3, 42.71/57.29 and 52.65/47.35 at ammonia concentration of 14.0, 11.0 and 8.0 M, respectively which mean a better stoichiometric ratio at low ammonia concentration is obtained. Hasnet et al reported that the quantitative results of pure CdS thin film from EDX analysis yielded a Cd to S ratio equal to 1.09 suggesting the presence of sulphur vacancies (excess of cadmium) in the deposited films, which act as donors, leading to n-type conductivity [19-20].

3.1.3 Effect of thiourea concentration

Figure (4) presents the SEM micrographs of the surface morphology of CdS films deposited with different thiourea concentrations (0.06M and 0.09M). With the lower thiourea concentration the small particles accumulate continuously and cover the entire surface of the substrate leading to an homogeneous layer the average crystallite size of these films varies between 2.9 to 7.6 μm . This indicates that the mechanism film formation is due to ion-by-ion deposition (heterogeneous mechanism). At higher thiourea concentration a small particles are grouped to form larger clusters discretely distributed in the films as it is shown clearly. This indicates that the mechanism film formation is due to cluster-by-cluster deposition (homogeneous mechanism). The average crystallite size of these films varies between 7.5 to 13.4 μm . It is revealed that increasing of the grain size at high concentration of 0.09M thiourea makes the CdS layer denser and the granules formed a cluster shape with large grains and a few defects, show a good adhesion to the FTO substrate. The EDX analysis for the CdS films prepared with the different thiourea concentrations are summarized as follows. S/Cd ratios are 45.7/54.3 and 48.67/51.3 at 0.06M and 0.09M, respectively. Cadmium and sulfur are believed to form the solid solution in the electrolyte and hence the composition of the film is expected to depend on the concentration of chemicals dissolved in the electrolyte. The films are found to be composed of cadmium and sulfur without any foreign impurity. It can be concluded that the film became

cadmium-rich with decreasing concentration of thiourea. A satisfactory stoichiometry is achieved for 0.09M of thiourea. A close result was achieved by Chaure et al where they found that this ratio was obtained at 0.13M thiourea [21].

3.2 Crystalline structure of CdS Film

Figure (6) presents the x-ray diffraction patterns of CdS layers deposited with 1, 2 and 6 successive stages. The XRD analysis shows that the CdS films have highly oriented crystallites with the classical hexagonal structure (wurtzite type) and the main six diffraction peaks are corresponded to (100), (002), (101), (102), (110) and (103) planes. This is matched with the JCPDS card no. 41-1049 [25]. The intensities of diffracted peaks increase with the rising the number of successive deposition stages. The intensity of the peaks shows that one deposition stage is poorly crystallized, while the intensities of the peaks are improved at 2 deposition stages indicating. If we compare the XRD patterns of CdS film formed with 2 stages with CdS film deposited with 6, we found that intensity of plane (100) is enhanced by 36%, plane (002) increases by 68%, plane (102) is improved by 32% and there are no change in intensities of the planes of (110) and (103). It can conclude that preferential orientation of crystallites of CdS film is (002). The relatively stronger and narrow peak of CdS film obtained with 6 stages along (002) plane indicates that the film is highly oriented along the c-axis. This suggests that CdS film deposited with 6 stages of is well crystallized and the increase in intensity of the crystalline peaks with the number of deposition stages is due to the increase of the film thickness [26].

3.3 Optical Analysis of CdS

The optical transmission spectrum of the CdS film between 490 to 720 nm was used to obtain CdS band gap. Figure (7) illustrates the plot of $(\alpha h\nu)^2$ vs. $h\nu$ of the CdS film deposited with one stage. It has been observed that the plot of $(\alpha h\nu)^2$ versus $h\nu$ is linear over a wide range of photon energy indicating a specific type of transition. The intercept (extrapolation) of the plot (straight line) on the energy axis reflects the energy band gap. The band gap E_g can be extrapolated to be 2.41 eV. The thickness, refractive index and the absorption coefficient α of thin films calculated by the Swanepoel model, using the following equations [27-28]:

$$n = [N + (N^2 + n_s^2)^{1/2}]^{1/2} \quad (1)$$

$$N = 2n_s \frac{T_M - T_m}{T_M T_m} + \frac{n_s^2 + 1}{2} \quad (2)$$

$$d = \frac{\lambda_1 \lambda_2}{2(\lambda_1 n_2 - \lambda_2 n_1)} \quad (3)$$

$$\alpha = \frac{1}{d} \ln \frac{(n-1)(n-n_s) \left(\frac{T_M}{T_m} + 1\right)^{1/2}}{(n+1)(n+n_s) \left(\frac{T_M}{T_m} - 1\right)^{1/2}} \quad (4)$$

where n is the refraction indices at various wavelengths, T_M and T_m are the maximum and minimum transmissions at specific wavelength λ and n_s is the refractive index of the substrate ($n_s=1.52$ for glass). n_1 and n_2 are the refractive indices at two adjacent max or min at λ_1 and λ_2 , h is Planck constant and ν is the photon's frequency. The calculated average thickness, and refractive index were $0.91 \mu\text{m}$, and 2.46 respectively.

3.4 Performance of FTO / CdS /CdTe / Mo X-Ray Detector

Figures (8) shows output signal from FTO/CdS/CdTe/Mo detector exposed to x-ray of 21, 27 and 30 keV at 0.05mA intensity. It is observed that the maximum amplitudes of the pulse formed due to exposed FTO/CdS/CdTe/Mo detector to X-ray are 0.41, 065 and 0.72V respectively, at 39 KeV any further increase in X-ray energy cause very slight increase in signal amplitude. Figure (9) shows output signal from FTO/CdS/CdTe/Mo detector exposed to x-ray of 21, 27 and 33 keV at 1mA intensity. It is observed that the maximum amplitudes of the pulse formed due to exposed FTO/CdS/CdTe/Mo detector to X-ray are 0.64, 0.86 and 1.03V respectively, any increase in X-ray energy beyond 33KeV cause very slight change in the pulse amplitude. The produced peaks with X-ray exposure can be explained by assumption of electrical circuit. R represents the input resistance of the circuit and C represents the equivalent capacitance of both the FTO/CdS/CdTe/Mo detector and the measuring circuit. The time-dependent voltage $V(t)$ across the load resistance is the fundamental signal voltage output, the pulses which their amplitudes depend on the amount collected charges and relative value of the time constant of the measuring circuit. The time

constant equals to RC . If the time between pulses is sufficiently large, the capacitance will discharge through the resistance and the voltage across the load resistance returns to zero. So the time required for the signal pulse to reach its maximum value is determined by the charge collection time within the FTO/CdS/CdTe/Mo detector. The time required to restore the signal voltage to zero is determined by the time constant of the load circuit. The amplitude of the signal pulse is determined by the ratio of the total charge created within the detector during one radiation interaction divided by the capacitance of the equivalent load circuit. Because the capacitance is fixed, the amplitude of the signal pulse is directly proportional to the generated charge [29]. The signal formation is through three steps. In step (1), is the formation of depletion region or junction prevents the passing of the free charges from the bulk. In step (2), X-ray passes through the FTO/CdS/CdTe/Mo detector where the most interaction occurred in the CdS/CdTe junction. X-ray photons are disappeared and a photoelectron produced from one of the electron shells of the absorber CdS/CdTe junction with kinetic energy equals the incident photon energy minus the binding energy of the electron in its original shell. The vacancy that is created in the electron shell as a result of the photoelectron emission is quickly filled by electron rearrangement where a characteristic X-ray is produced. X-rays reabsorbed again through photoelectric interactions with less tightly bound electron shells of the CdS/CdTe junction. In step (3), the produced electrons cause the appearance of a given amount of electric charge within the detector. These created charges flow in the opposite directions and collected at the electrodes causing electrical pulses.

Figure (10) shows the output signal of FTO/CdS/CdTe/Mo detector versus X-ray energy at different intensities. The amplitude is linearly increased with energy of X-ray until 33 keV then there is a very slight increase in the signal amplitude. The electron-hole pairs produced from high energy X-ray are far from the junction of the detector and consequently the recombination process of electron-hole pairs is dominant. We can conclude that the linearity of the FTO/CdS/CdTe/Mo detector is better at lower intensity of X-ray than obtained at higher intensity [30]. Shin Watanabe developed two prototype models of the CdTe stacked detector which consists of 10 and 40 CdTe detectors. Each diode has

an area of 21.5 mm × 21.5 mm and a thickness of 0.5 mm. A bias voltage of 300 V was used. The 10 layer module was used to measure the spectrum of ⁶⁰Co which radiate gamma ray with energy 1173 keV and 1332 keV. The 40 layer module used to measure the higher energy source ²⁵²Cf which produce neutrons with energy 5100, 5600 and 6100 keV. The idea of plural planer detectors with the high thickness of detector increased the probability of interaction which make the detector can detect gamma ray and neutron in the energy range from 1.17 to 5.6 MeV [31]. In our work we used the energy range from 21 to 42 keV because the maximum obtained thickness for CdS/CdTe junction is 6.8 μm. The stacked 4 CdS/CdTe junction increases the area of the detector. As the area increases, the number of interactions of X-ray with CdS/CdTe junction increases resulting the increase in the collected charge and the signal amplitude.

4 Conclusion

Multilayer of CdS using CBD were succeeded to deposit thick layer to fabricate FTO/CdS/CdTe/Mo X-ray detector. The optimal concentrations were found to be 0.09 M and 8 M for thiourea and ammonia, respectively, while the optimum deposition time was 4 hours with 1 N CdCl₂ with heat treatment at 350°C for 15 min. These optimal deposition parameters were used to produce thick film by depositing 6 successive thin films. The side view SEM indicated that 6 stages deposition of CdS layers yielded 2.8 μm. CdTe was electrodeposited onto the prepared CdS/FTO substrates. The cyclic voltammetry was used to provide the optimum applied voltage for CdTe deposition onto CdS/FTO glass substrate, where -1.2 V was found suitable for CdTe film deposition. By growing CdTe layer onto CdS/FTO at constant voltage a homogeneous good distribution layer was established with maximum thickness 4 μm. Mo metal as a back contact was deposited on CdTe/CdS/FTO hetero junction samples by DC magnetron sputtering system. The performance of the FTO/CdS/CdTe/Mo X-ray detector was measured by computerized oscilloscope. The output electric were measured at 21, 27 and 30 keV and 0.05 mA intensity and were found to be 0.41, 0.65 and 0.72V respectively, while the peak amplitude at 21, 27 and 33 keV and 1mA intensity were found to be 0.64, 0.86 and 1.13V respectively, which indicating good performance, response and

sensitivity to different X-ray energy and intensity. By utilizing peak amplitude obtained from the detector, we demonstrate a new method to measure X-ray with the 4 detector stacked in series. Stacked FTO/CdS/CdTe/Mo X-ray detector have been developed, demonstrating room-temperature semiconductor radiation detectors. The used fabrication method intended to be simple, low cost and available to reduce the production cost of the detector. This new detector technology is useful for many applications requiring direct, high sensitive imaging of X-rays at room-temperature.

References:

- [1] R.S. Mane, and C.D. Lokhande, Chemical deposition method for metal chalcogenide thin films, *Materials Chemistry and Physics* I-31, 65 (2000)
- [2] H. Khallaf, Isaiah O. Oladeji, G. Chai, and L. Chow, Characterization of CdS thin films grown by chemical bath deposition using four different cadmium sources, *Thin Solid Films* 7306–7312, 516 (2008).
- [3] S. Wagner, J. L. Shay, P. Migliorato, and H. M. Kasper, *CuInSe₂/CdS heterojunction photoVoltaic detectors*, (1974) <https://doi.org/10.1063/1.1655537>
- [4] Y. Tomita, Y. Hatanaka, T. Takabayashi, and T. Kawai, *X-Ray Imaging Camera Tube Using Sputter-Deposited CdTe/CdS Heterojunction*, (1993) <https://doi.org/10.1109/16.182507>
- [5] J. W. Murphy, J. W., L. Smith, J. Calkins, and G. R. Kunnen, (2014), *Thin Film Cadmium Telluride Charged Particle Sensors for Large Area Neutron Detectors*, <https://doi.org/10.1063/1.4895925>.
- [6] J. Kang, E. I. Parsai, D. Albin, V. G. Karpov, and Diana Shvydka, *From photovoltaics to medical imaging: Applications of thin-film CdTe in x-ray detection*, (2008) <https://doi.org/10.1063/1.3042212>.
- [7] M Ilieva, D. Dimova Malinovska, B. Rangelov and I Markov, *High temperature electrodeposition of CdS thin films on conductive glass substrates*, *Condens. Matter* 10025–10031, 11 (1999).
- [8] A. Palafox, G. R. Paredes, A. Maldonado, R. Asomoza, D.R. Acosta, and J. Palacios-Gomez, *Physical properties of CdS and CdS : In thin films obtained by chemical spray over different*

- substrates, *Solar energy Materials and Solar Cells*. 31-41, 55 (1998).
- [9] P. Boieriu, R. Sporcken, Y. Xin, N.D. Browning, and S. Sivananthan, *Wurtzite CdS on CdTe Grown by Molecular Beam Epitaxy*, (1999) <https://doi.org/10.1007/s11664-000-0212-3>.
- [10] H. Uda, H. Yonezawa, Y. Ohtsubo, M. Kosaka, and H. Sonomura, *Thin CdS films prepared by metalorganic chemical vapor deposition*, *Solar Energy Materials and Solar Cells* 219–226, 75 (2003).
- [11] M. Sasagawa, and Y. Nosaka, *The effect of chelating reagents on the layer-by-layer formation of CdS films in the electroless and electrochemical deposition processes*, *Electrochimica Acta* 483-488, 48 (2003).
- [12] B. E. Mcandless, I. Youm, and R. W. Birkmire, *Optimization of Vapor Post-Deposition Processing for Evaporated CdS/CdTe Solar Cells*, (1999) [https://doi.org/10.1002/\(SICI\)1099-159X\(199901/02\)7:1<21::AID-PIP244>3.0.CO;2-D](https://doi.org/10.1002/(SICI)1099-159X(199901/02)7:1<21::AID-PIP244>3.0.CO;2-D).
- [13] M.A. Islam, M.S. Hossain, M.M. Aliyu, P. Chelvanathan, Q. Huda, M.R. Karim, K. Sopian, and N. Amin, *Comparison of Structural and Optical Properties of CdS Thin Films Grown by CSVT, CBD and Sputtering Techniques*, *Energy procedia* 203 – 213, 33 (2013).
- [14] S. Ramprasad, Y. Su, C. Chang, B. K. Paul, D. R. Palo, *Cadmium sulfide thin film deposition: A parametric study using microreactor-assisted chemical solution deposition*, *Solar Energy Materials and Solar Cells* 77–85, 96 (2012).
- [15] I. O. Oladej, and L. Chow, *Optimization of Chemical Bath Deposited Cadmium Sulfide Thin Films*, (1997) <https://doi.org/10.1149/1.1837815>
- [16] D. H. Rose and F. S., *Fabrication Procedures and process Sensitivity for CdS/CdTe Solar Cells*, *Photovolt: Res. Appl.*, 331-340, 7 (1999).
- [17] F. Ouachtari, A. Rmili, S. El Bachir, A. Bouaoud, H. Erguig, and P. Elies, *Influence of Bath Temperature, Deposition Time and [S]/[Cd] Ratio on the Structure, Surface Morphology, Chemical Composition and Optical Properties of CdS Thin Films Elaborated by Chemical Bath Deposition*, *Modern Physics*, 1073-1082, 2 (2011).
- [18] M. Reddy, and N. Vara, *Properties of CdS Chemically Deposited thin films on the Effect of Ammonia Concentration*, *IOSR Applied Physics* 2278-4861, 4 (2013).
- [19] A. Hasnat and J. Podder, *Optical and Electrical Characteristics of Pure CdS Thin Films for Different Thicknesses*, *Bangladesh Academy of Sciences*, 33-41, 1 (2013).
- [20] R. J. Xavier, A. J. Amalraj, and V. Dharmalingam, *Effect of Ammonia concentration on structural and optical properties of CdS thin films prepared by CBD method*, *Chem. Tech. Research*, 0974-4290, 3 (2017)
- [21] S. Chaure, N.B. Chaure, R.K. Pandey and A.K. Ray, *Stoichiometric effects on optical properties of cadmium sulphide quantum dots*, (2007) <https://doi.org/10.1049/iet-cds:20070048>.
- [22] K. Mokurala, L. L. Baranowski, F. Willian, S. Siol, M. Van Hest, S. Mallick, P. Bhargava, and A. Zakutayev, *Combinatorial chemical bath deposition of CdS contacts for chalcogenide photovoltaics*, (2016) <https://doi.org/10.1021/acscmbosci.6b00074>.
- [23] J. N. Alexander, S. Higashiya, D. Caskey, H. Efstathiadis, and P. Haldar, *Deposition and characterization of cadmium sulfide (CdS) by chemical bath deposition using an alternative chemistry cadmium precursor*, (2014) <https://doi.org/10.1016/j.solmat.2014.02.017>
- [24] F. Lisco P.M. Kaminski, A. Abbas, K. Bass, J.W. Bowers, G. Claudio, M. Losurdo, J.M.Walls, *The structural properties of CdS deposited by chemical bath deposition and pulsed direct current magnetron sputtering*, (2014) <https://doi.org/10.1016/j.tsf.2014.11.062>.
- [25] Weizhi Wang, Yajing Lu, Yafei Xu, Konglin Wu, Jiarui Huang, Changchun Jia and Si Ok Ryu, *A facile template-free approach for fabrication of flower-like CdS: the evolutionary process of the structure and the performance of photocatalytic activity*, *Royal society journal of chemistry*, (2016) <https://doi.org/10.1039/c6ce00025h>.
- [26] A. Nawaz, Z. Rabeel and N. A. Shah, *Investigations on the Physical Properties of CdCl₂ Heat-Treated ITO/CDTE/CDS Thin Films Solar Cell*, (2014) <https://doi.org/10.5829/idosi.wasj.2014.31.08.621>.
- [27] J. C. Manificier, J. Gasiot and J. P. Fillard, *A simple method for the determination of the optical constants n, h and the thickness of a weakly absorbing thin film*, (1976) <https://doi.org/10.1088/0022-3735/9/11/032>.

- [28] S. ilican, M. Caglar, and Y. Caglar, Determination of the thickness and optical constants of transparent indium-doped ZnO thin films by the envelope method, *Material Science-Poland*, 0137-1339, 3 (2007).
- [29] G. E. Knoll. *Radiation Detection and Measurement* 3rd edn., (John Wiley and Sons, New York, 2000) (PP. 48:53, 103:111, 308:317).
- [30] J. Abramovitch, Engaged learning at SMUD digital repository, Development of a Silicon PIN Diode X-Ray Detector (2014), http://digitalrepository.smu.edu/upjournal_research/32.
- [31] S. Watanabe, T. Takahashi, K. Nakazawa, Y. Kobayashi, Y. Kuroda, K. Genba, M. Onishi, and K. Otake, A Stacked CdTe Gamma-ray Detector and its application as a range finder, (2003) [https://doi.org/10.1016/S0168-9002\(03\)01032-5](https://doi.org/10.1016/S0168-9002(03)01032-5).

Appendix

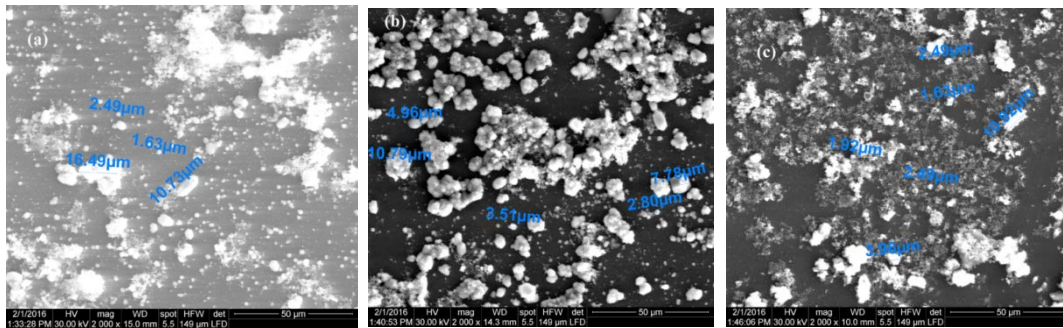


Figure : 2 SEM micrographs of CdS films deposited with different deposition times: (a)2hours, (b)3hours, (c)4hours.

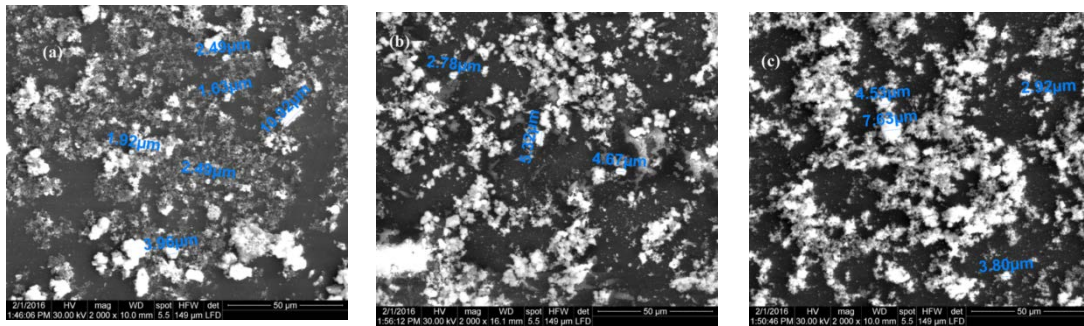


Figure : 3 SEM micrographs of CdS thin films deposited with different NH3OH concentrations: (a)14M ,(b)11M ,(c)8M.

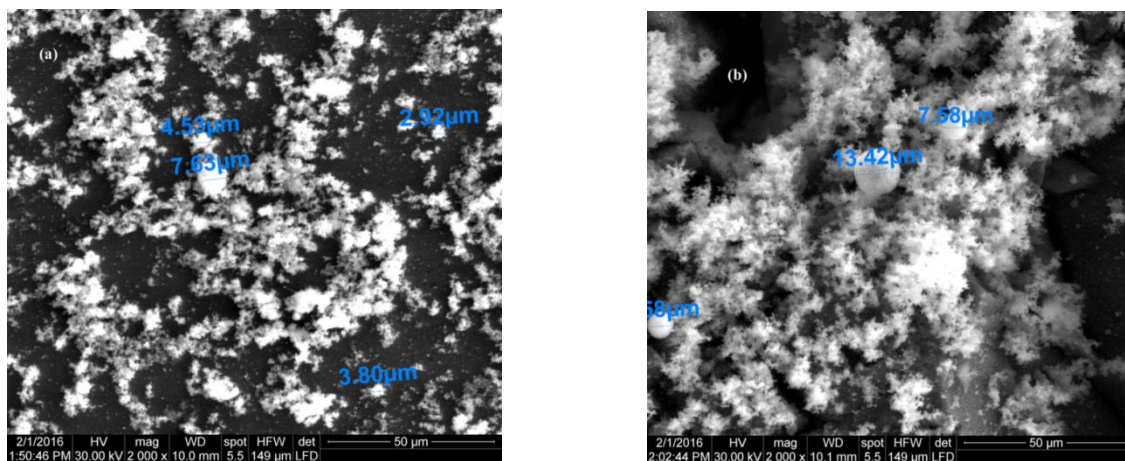
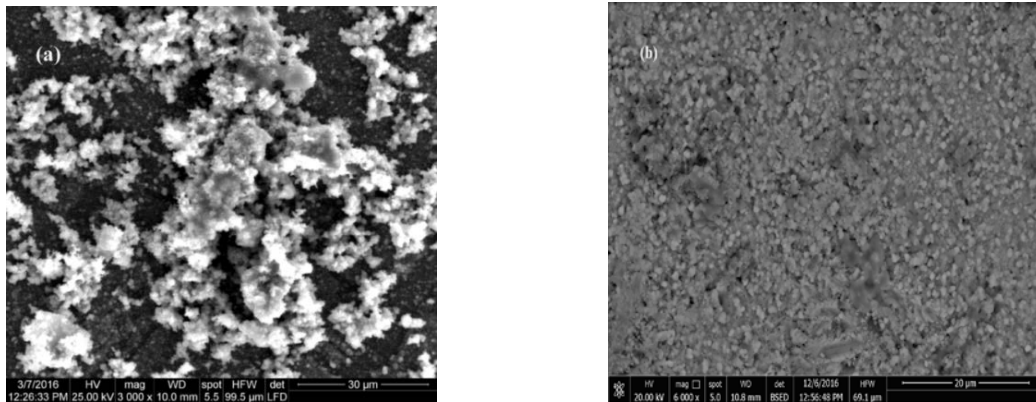


Figure : 4 SEM micrographs of CdS thin films deposited with different thiourea concentrations: (a) 0.06M, (b) 0.09M.

Top surface



Cross section

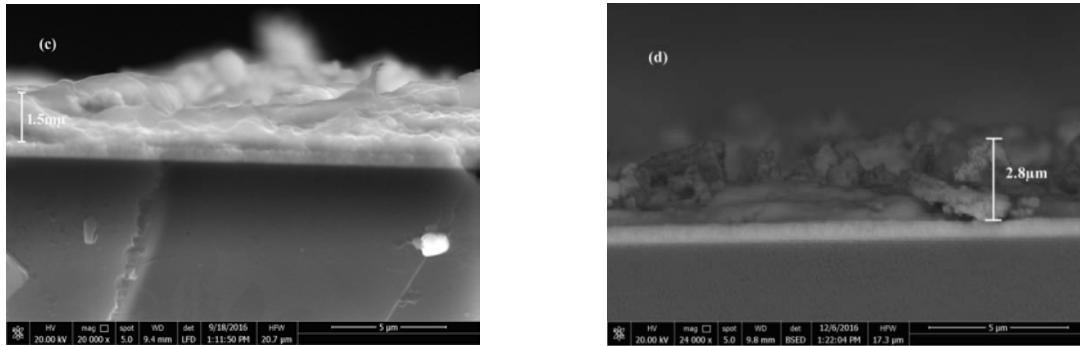


Figure (5) SEM micrographs top surface of CdS films deposited (a) 2 stages, (b) 6 stages

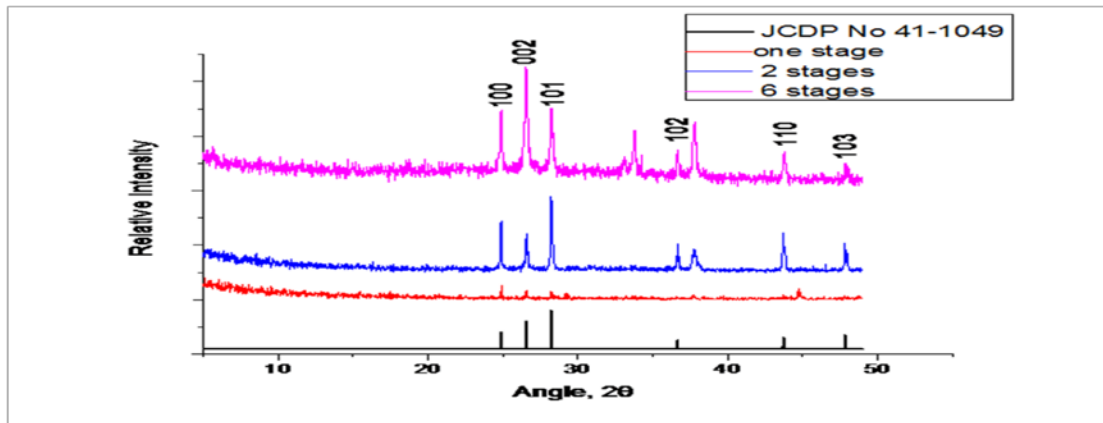


Figure (6) X-ray diffraction patterns of CdS thin films deposited one stage, 2 stages and 6 stages.

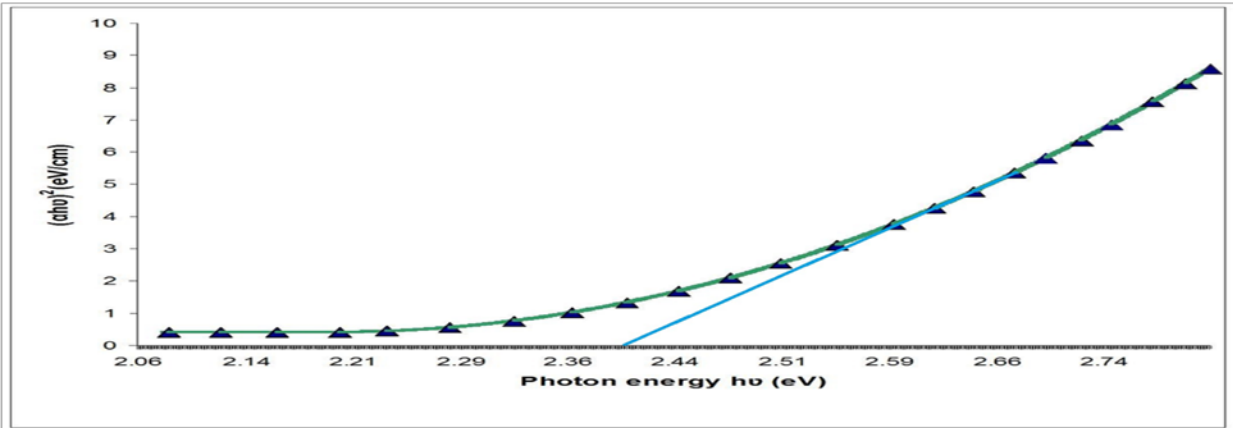


Figure : $7 (\alpha h\nu)^2$ versus $h\nu$ of CdS deposited film using one stage method.

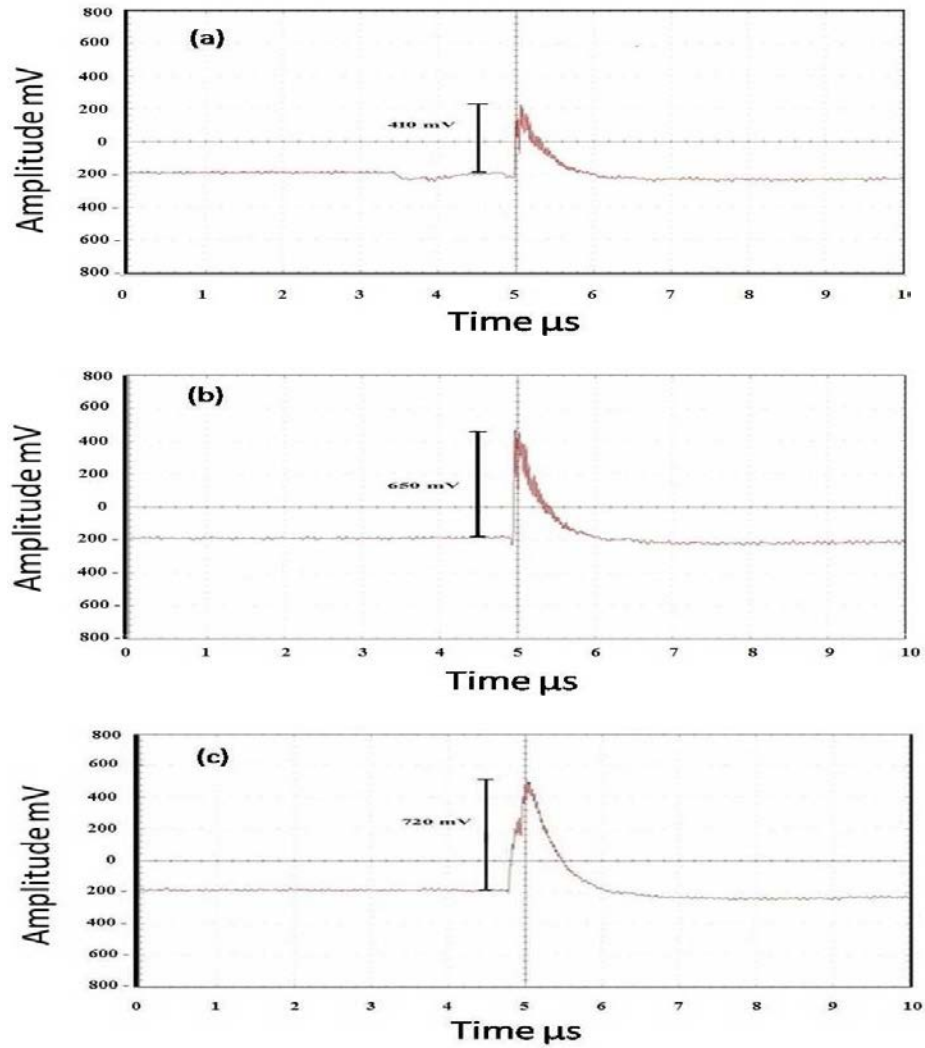


Figure 8: Output signal of sensor exposed to X-ray 0.05 mA intensity and energy (a) 21 keV (b) 27 keV (c) 30 keV.

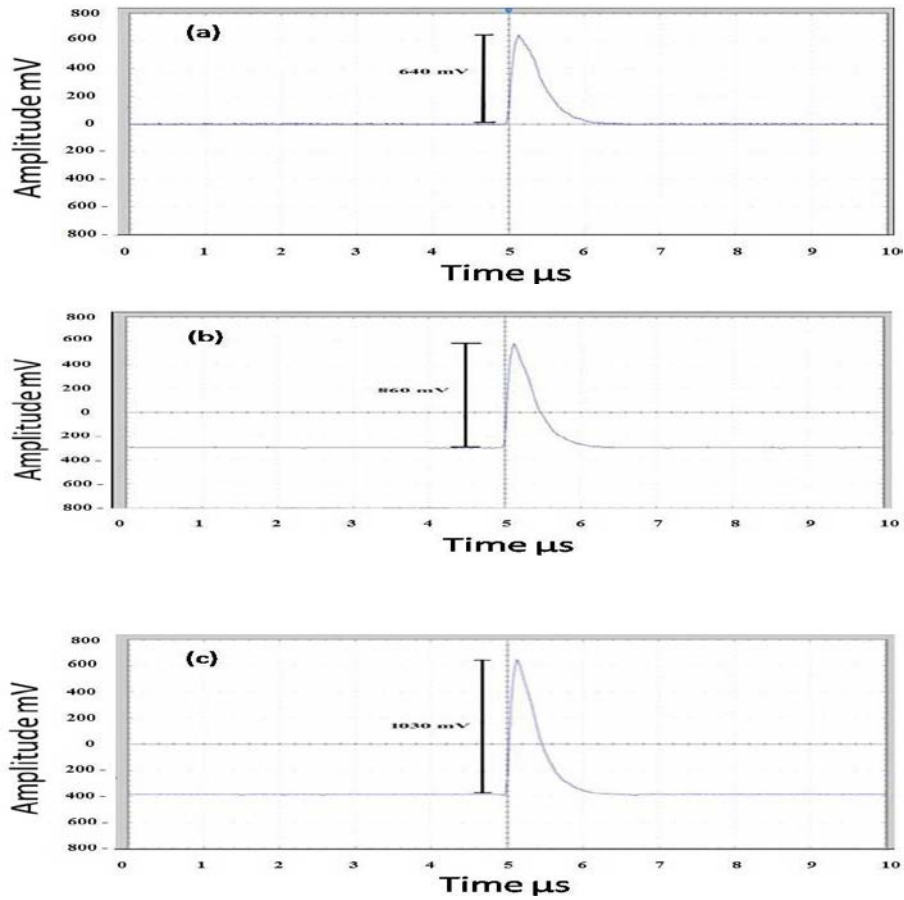


Figure 9: Output signal of sensor exposed to X-ray 1mA intensity and energy (a) 21 keV (b) 27 keV (c) 33 keV.

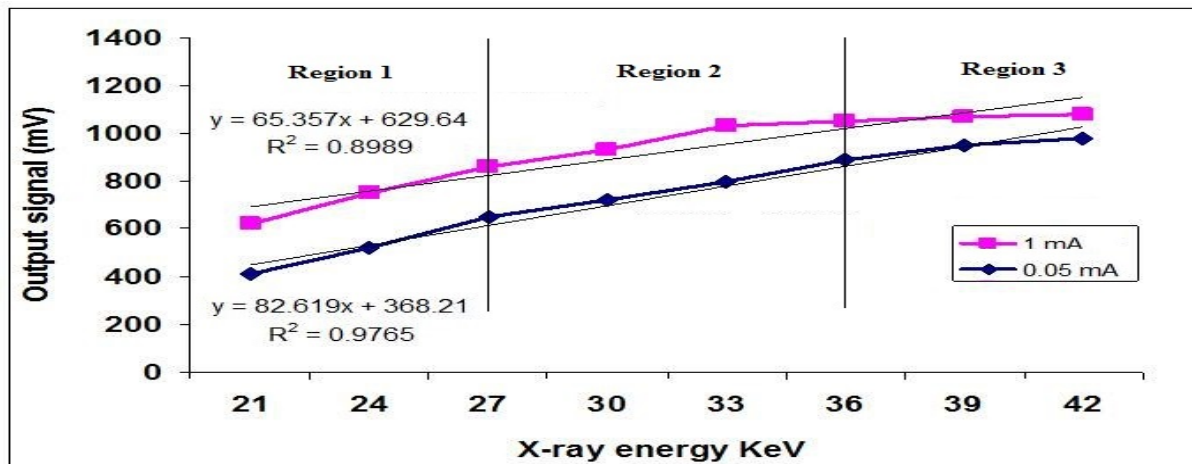


Figure 10: Output signal amplitude of FTO/CdS/CdTe/Mo sensor versus X-ray energy at different intensities.